Aerospace Engineering Communications
http://dx.doi.org/10.62762/AEC.2026.595594

RESEARCH ARTICLE

Communication Topology Resilience-Guided Optimization for Multi-UAV Cooperative Planning

Quan Li[1], **Zitong Shen**[1], **Qingwen Ding**[1], **Yaxuan Liu**[1,*], **Rui Dai**[2], **Jin Zhou**[1] **and Yiyang Ni**[1]

[1] School of Computer Engineering and School of Artificial Intelligence, Jiangsu Second Normal University, Nanjing 210013, China

[2] College of Artificial Intelligence, Jiaxing University, Jiaxing 314001, China

Abstract

This paper studies cooperative mission planning for multi-unmanned aerial vehicle (UAV) swarms in obstacle-cluttered environments, with particular attention to mission feasibility and communication-topology resilience. Considering that task assignment and waypoint selection directly affect the inter-UAV communication graph, a communication topology resilience-guided (CTR) method is proposed by introducing algebraic connectivity as an explicit topology metric. The method first performs topology-guided one-to-one task assignment using simulated annealing, jointly considering normalized distance, obstacle risk, and algebraic connectivity. It then selects topology-aware key waypoints according to path length, obstacle risk, isolation penalty, and conflict-neighborhood cost, followed by path stitching and wait-insertion-based temporal conflict correction. Compared with prioritized planning (PP) and genetic algorithm (GA) baselines, CTR achieves a higher mission success rate and stronger algebraic connectivity, while substantially improving communication connectivity over the topology-ablated variant with essentially the same success rate. Monte Carlo simulations under different swarm sizes and obstacle densities verify the effectiveness of the proposed method.

Keywords: multi-UAV swarm, cooperative planning, communication topology resilience, algebraic connectivity, simulated annealing.

1 Introduction

Unmanned aerial vehicle (UAV) swarms are attractive for missions that demand large-area coverage, rapid deployment, and parallel execution, such as search and rescue, regional inspection, and cooperative mapping [1]. Compared with single-UAV path planning, swarm planning must coordinate multiple UAVs under shared spatial and temporal constraints, which couples task assignment, path generation, and inter-UAV collision avoidance [2]. Existing multi-agent path-finding methods mostly address graph search, priority-based planning, and centralized conflict resolution [3, 4]. Among them, prioritized planning (PP) [4] plans each agent sequentially in a

Submitted: 20 July 2026
Revised: 21 September 2026
Accepted: 23 September 2026
Published: 26 September 2026

Vol. 1, **No.** 3, 2026.
10.62762/AEC.2026.595594

***Corresponding author:**
Yaxuan Liu
carol_liuyx@163.com

Citation
Li, Q., Shen, Z., Ding, Q., Liu, Y., Dai, R., Zhou, J., & Ni, Y. (2026). Communication Topology Resilience-Guided Optimization for Multi-UAV Cooperative Planning. *Aerospace Engineering Communications*, 1(3), 128–136.

fixed priority order, while genetic algorithms (GAs) [5, 6] perform population-based assignment optimization. We adopt both as representative classical baselines. Optimal search-based solvers such as conflict-based search (CBS) [7] resolve inter-agent conflicts with optimality guarantees, but their computational cost grows rapidly with the number of agents and conflicts. In complex obstacle environments, however, simultaneously ensuring mission success, collision safety, and computational efficiency remains difficult.

Most prior studies treat task assignment and trajectory generation separately. Auction-based and consensus-based assignment methods [8] are efficient but rarely account for how the resulting spatial configuration affects the swarm communication graph. Distributed connectivity-maintenance controllers have been developed for mobile multi-agent networks [9], but they act at the motion-control level and do not influence which targets are assigned. Learning-based planners [10–13] can adapt to environments but usually encode safety as a reward term without an explicit connectivity objective. In networked control, agent positions have also been optimized to maximize the algebraic connectivity of a state-dependent graph Laplacian [14], which motivates using λ_2 as a planning objective. A few recent works couple UAV trajectory design or task coordination with communication awareness [15–18], yet the communication requirement is often imposed as a hard constraint or a per-link reward rather than as a global resilience metric. Combinatorial task-assignment problems are commonly solved by metaheuristic optimization methods such as simulated annealing (SA) [19], and pairwise communication costs can be cast as a quadratic unconstrained binary optimization (QUBO) problem. Unlike pairwise communication costs, however, the algebraic connectivity is a spectral (nonlinear) function of the assigned configuration. We therefore evaluate the topology term directly inside the SA search, which requires only an objective evaluation rather than a QUBO reformulation.

In this paper, we propose a communication topology resilience-guided (CTR) method for multi-UAV cooperative planning. The main contributions are threefold.

1. The swarm communication topology is modeled as a weighted graph whose resilience is quantified by the algebraic connectivity λ_2; this scalar is used as a global objective rather than a collection of per-link constraints.

2. A topology-guided task assignment stage is formulated: a spectral objective combining a distance-normalized risk cost with an algebraic-connectivity reward is minimized by simulated annealing under one-to-one matching, so that the assigned targets jointly strengthen the swarm connectivity.

3. A topology-aware waypoint selection stage is formulated: each UAV chooses a key waypoint from a candidate set by directly minimizing a cost that embeds an isolation-penalty topology cost together with path-length, obstacle-risk, and conflict-neighborhood costs; A* stitching and wait insertion are subsequently used to generate collision-free and temporally consistent trajectories when a feasible solution is found.

Simulation results show that CTR attains the highest algebraic connectivity, together with a higher success rate than PP and GA; ablating the topology terms sharply degrades connectivity while leaving the average success rate essentially unchanged, under three swarm sizes and three obstacle densities.

The rest of this paper is organized as follows. Section 2 presents the problem formulation and the communication topology model. Section 3 introduces the proposed CTR method. Section 4 presents the simulation results and analysis. Section 5 concludes this paper.

2 Problem Formulation and Communication Topology Model

2.1 Problem Description

Consider N UAVs in a 2-D grid world with dimensions $W \times H$. The M targets $(M \geq N)$ form a candidate task pool, and each planning instance selects and assigns exactly N targets according to the available swarm capacity. The i-th UAV starts from $s_i \in \mathbb{Z}^2$ and must reach its assigned target $g_i \in \mathbb{Z}^2$ while avoiding static obstacles and maintaining a minimum inter-UAV separation $d_{\min}$. The desired planning output is a set of collision-free paths $\{P_i\}$, where each path is a sequence of grid cells. The objectives are (i) mission success, (ii) collision safety, (iii) communication topology resilience, and (iv) path efficiency.

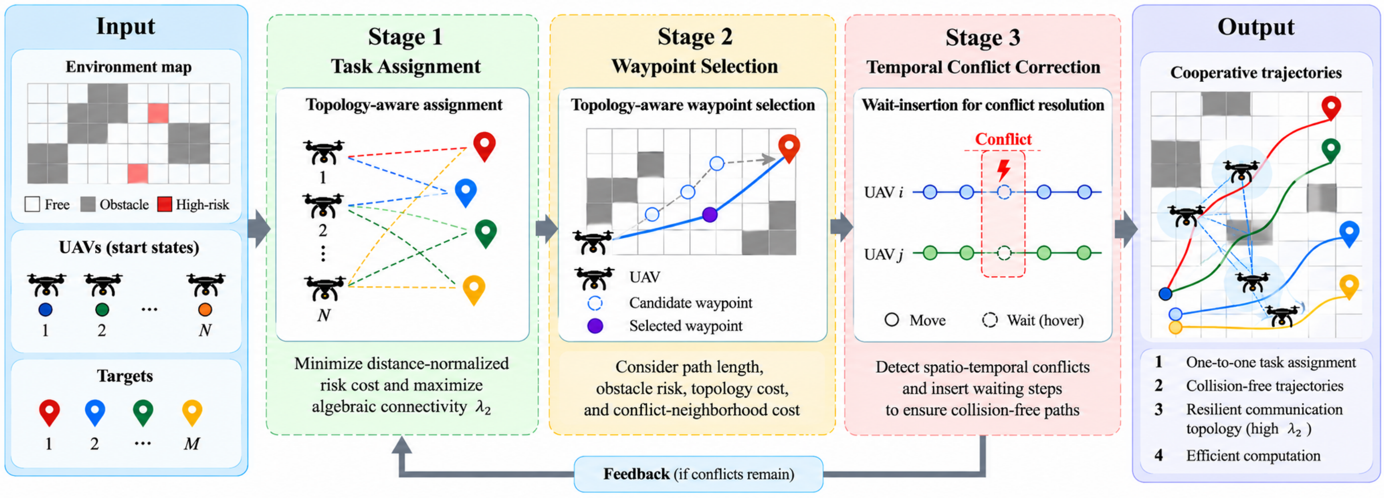

Figure 1. Overview of the proposed CTR framework: a topology-guided task assignment stage (simulated annealing) and a topology-aware waypoint selection stage are followed by A* path stitching and wait-insertion temporal conflict correction.

2.2 Communication Graph and Algebraic Connectivity

Let the instantaneous position of UAV i be p_i. The inter-UAV communication graph is encoded by a weighted adjacency matrix whose entries decay with distance within a communication radius R_c:

$$a_{ij} = \begin{cases} \exp(-d_{ij}/R_c), & i \neq j \text{ and } d_{ij} \leq R_c, \\ 0, & \text{otherwise}, \end{cases} \tag{1}$$

where $d_{ij} = \|p_i - p_j\|$. No self-loops are included, i.e., $a_{ii} = 0$ for all i. The degree matrix is $D = \operatorname{diag}(\sum_j a_{ij})$, and the graph Laplacian is

$$L = D - A. \tag{2}$$

Let $0 = \lambda_1 \leq \lambda_2 \leq \cdots \leq \lambda_N$ be the eigenvalues of L. The second smallest eigenvalue λ_2, known as the algebraic connectivity [20], satisfies $\lambda_2 > 0$ if and only if the graph is connected. Larger λ_2 indicates a more robustly connected topology [21]. For the weighted graph considered here, where the edge weights satisfy $0 \leq a_{ij} \leq 1$, Fiedler's bound $\lambda_2 \leq \frac{N}{N-1} \min_i \sum_j a_{ij} \leq N$ gives $\lambda_2 \leq N$, and we therefore use the normalized topology cost

$$J_T(\mathcal{G}) = 1 - \frac{\lambda_2(L(\mathcal{G}))}{N} \in [0, 1], \tag{3}$$

where $\mathcal{G}$ denotes the weighted communication graph and $L(\mathcal{G})$ is its Laplacian matrix. Minimizing J_T drives the swarm toward a better-connected topology. In this work, topology resilience is characterized through the algebraic connectivity as a surrogate measure of connectivity robustness.

3 Proposed CTR Method

The proposed CTR framework comprises two topology-aware planning stages followed by temporal conflict correction, as summarized in Algorithm 1 and illustrated in Figure 1.

3.1 Topology-Guided Task Assignment via Simulated Annealing

The assignment of N UAVs to M targets is encoded by binary variables $x_{ij} \in \{0, 1\}$, where $x_{ij} = 1$ if UAV i is assigned to target j. In all experiments the task pool contains $M = 2N$ targets, of which exactly N are assigned one-to-one to the UAVs; the remaining $M - N$ targets are left unassigned. The linear cost combines a normalized distance and an obstacle-risk term:

$$c_{ij} = \frac{\|s_i - g_j\|}{L_{\text{ref}}} + \gamma_r \frac{1}{\max(\rho(g_j), 1)}, \tag{4}$$

where $\rho(q)$ denotes the Manhattan distance (in grid cells) from cell q to the nearest occupied obstacle cell, and γ_r is the risk weight. A feasible one-to-one assignment is maintained by the SA move operators: at each iteration a UAV is either reassigned to a free target or swaps targets with another UAV. Because the algebraic connectivity is a spectral (nonlinear) function of the selected target configuration, it cannot be expressed as a quadratic form in x; the assignment objective is therefore evaluated directly by SA rather

Algorithm 1: CTR cooperative planning

Input: world, starts S, task pool $\mathcal{T}$, config `cfg`
Output: feasible paths $\{P_i\}$, or failure
$N \leftarrow |S|$, $M \leftarrow |\mathcal{T}|$;
$L_{\mathrm{ref}} \leftarrow 2\sqrt{W^2 + H^2}$;
if *`cfg.assignment.enable`* **then**
  $\{g_i\} \leftarrow \mathrm{AssignTasksTopoSA}(S, \mathcal{T}, \texttt{cfg}, L_{\mathrm{ref}})$;
else
  $\{g_i\} \leftarrow$ index-order assignment of first N targets;
end
sort UAVs by distance to goal in ascending order;
for *each UAV i in order* **do**
  $reserved \leftarrow \mathrm{ReservedMask}(world, \{P\}, d_{\min})$;
  $C \leftarrow \mathrm{SampleCandidates}(world, s_i, g_i, reserved)$;

  if $C = \varnothing$ **then**
    return failure;
  end
  $m_i \leftarrow \arg\min_{c_k \in C} J(c_k)$;
  $P_{i,1} \leftarrow \mathrm{A}^*(s_i, m_i)$;
  $P_{i,2} \leftarrow \mathrm{A}^*(m_i, g_i)$;
  if *$P_{i,1}$ or $P_{i,2}$ is infeasible* **then**
    return failure;
  end
  $P_i \leftarrow P_{i,1} \oplus P_{i,2}$;
end
if *`cfg.deconflict.enable`* **then**
  $(\{P_i\}, status) \leftarrow \mathrm{DeconflictByWaiting}(\{P_i\}, \texttt{cfg})$;
  if *$status$ = failure* **then**
    return failure;
  end
end
return $\{P_i\}$;

than being cast as a QUBO:

$$\begin{aligned} \min_{\mathbf{x}} \quad & \sum_{i=1}^{N}\sum_{j=1}^{M} c_{ij}x_{ij} + w_T^{\mathrm{A}} J_T\big(\mathcal{G}(\mathbf{x})\big) \\ \text{s.t.} \quad & \sum_{j=1}^{M} x_{ij} = 1, \quad i = 1,\ldots,N, \\ & \sum_{i=1}^{N} x_{ij} \le 1, \quad j = 1,\ldots,M, \\ & x_{ij} \in \{0,1\}. \end{aligned} \tag{5}$$

where $\mathcal{G}(\mathbf{x})$ is the communication graph induced by the selected target set $\mathcal{T}(\mathbf{x}) = \{g_j : \sum_{i=1}^{N} x_{ij} = 1\}$, J_T is the normalized topology cost of (3) evaluated at those target positions, and w_T^{A} is the assignment-stage topology weight. These one-to-one constraints are preserved implicitly by the SA move operators described above. Starting from a greedy one-to-one matching based on c_{ij}, SA minimizes this combined cost, so the assignment jointly balances distance, obstacle risk, and the algebraic connectivity of the resulting target configuration. Note that the topology term depends only on the selected target subset $\mathcal{T}(\mathbf{x})$ and is invariant to how those targets are mapped to the UAVs, so the UAV-to-target correspondence is governed primarily by the distance-risk cost c_{ij}. A candidate move is accepted with probability

$$p_{\mathrm{acc}} = \min\Big(1, \exp(-\Delta J_{\mathrm{A}}/T_{\mathrm{SA}})\Big), \tag{6}$$

where ΔJ_{A} is the change in the assignment objective (5) induced by the move, and the temperature is updated as $T_{\mathrm{SA},k+1} = 0.995\, T_{\mathrm{SA},k}$. Unlike a pairwise range penalty, which over-punishes connected chains whose far-apart endpoints exceed R_c, this spectral term penalizes only configurations that weaken the global algebraic connectivity.

3.2 Topology-Aware Waypoint Selection

For each UAV i, a key waypoint is selected from a candidate set C containing up to K candidates sampled along the start–subgoal and subgoal–goal directions. The guidance subgoal is

$$\tilde{s}_i = s_i + \min\Big(12, \|g_i - s_i\|\Big)\frac{g_i - s_i}{\|g_i - s_i\|}, \tag{7}$$

rounded to the nearest grid cell; if that cell is occupied, the nearest free cell is used instead. This bounded stride prevents the subgoal from overshooting the target when the target lies within 12 cells of the start. The cost of candidate c is

$$\begin{aligned} J(c) = {} & w_L \frac{\|s - c\| + \|c - g\|}{L_{\mathrm{ref}}} + w_R \frac{1}{\max(\rho(c), 1)} \\ & + w_T^{\mathrm{W}} \tau(c) + w_C \frac{m(c)}{\eta}, \end{aligned} \tag{8}$$

where $s = s_i$ and $g = g_i$ are the start and assigned target of the UAV being planned, w_T^{W} is the waypoint-stage topology weight, and the topology term penalizes a candidate that would be isolated beyond R_c from every other predicted UAV position,

$$\begin{aligned} \tau(c) &= \min\Big(1, \max\Big(0, \frac{d_{\mathrm{near}}(c) - R_c}{R_c}\Big)\Big), \\ d_{\mathrm{near}}(c) &= \min_{j \ne i} \|c - \hat{p}_j\|, \end{aligned} \tag{9}$$

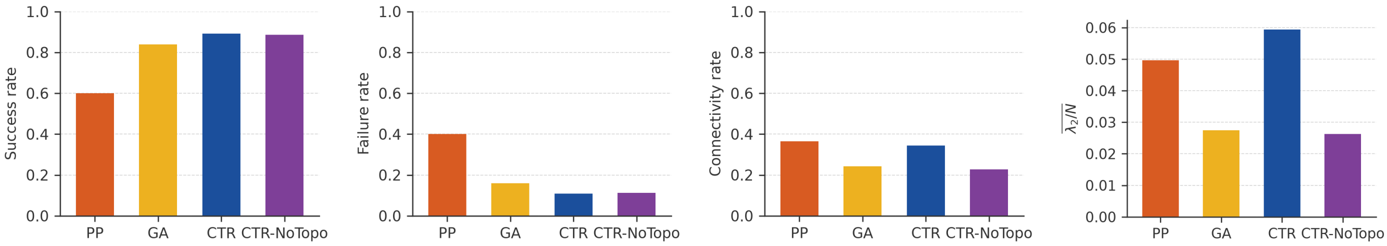

(a) Success (b) Failure (c) Connectivity (d) λ_2/N

Figure 2. Average (a) success rate, (b) failure rate, (c) connectivity rate, and (d) normalized algebraic connectivity across all swarm sizes and obstacle densities.

where $\hat{p}_j$ ($j \neq i$) are the predicted positions of the other UAVs, and $m(c) = \sum_{q \in \mathcal{N}_r(c)} \mathbf{1}_{\text{res}}(q)$ is the number of reserved cells within the $(2r+1) \times (2r+1)$ neighborhood $\mathcal{N}_r(c)$ centered at c, and $\eta = (2r+1)^2$ is the window size used for normalization. Staying within R_c of at least one neighbor incurs no penalty, which reduces the risk of isolated UAVs mid-flight without dragging all UAVs toward the swarm centroid and over-crowding the corridors; we emphasize that this local penalty does not guarantee global connectivity but serves as a computationally inexpensive surrogate for global connectivity that discourages fully isolated configurations. Since there are at most K candidates, the waypoint is selected by directly evaluating $J(c_k)$ and choosing the candidate with minimum cost; A* search then stitches the path through the selected waypoint. In Algorithm 1, $\oplus$ denotes path concatenation with the duplicated waypoint removed. The predicted positions of other UAVs use their already-selected waypoints if planned, and their guidance subgoals otherwise, which introduces a sequential dependence among the waypoint decisions through the isolation term.

3.3 Temporal Conflict Correction

Because spatial planning is sequential, synchronous execution may still create time-indexed collisions. A wait-insertion procedure scans the trajectories in time order, detects the earliest instant at which the inter-UAV separation drops below $d_{\min}$, and inserts waiting steps into the lower-priority path to remove that conflict. This scan-and-insert loop is repeated until no conflict is detected, up to a maximum of 400 iterations; if a conflict remains after this limit, the episode is declared failed. For successful episodes, this mechanism preserves the spatial paths while enforcing temporal safety.

4 Simulation Results

4.1 Setup

Experiments are conducted on a 100×100 grid containing $O \in \{10, 20, 30\}$ non-overlapping circular obstacles whose radii are drawn uniformly from $\{2, \ldots, 5\}$ cells. For each swarm size $N \in \{3, 5, 8\}$ and obstacle count O, the starts and a task pool of $M = 2N$ targets are drawn uniformly as collision-free grid cells separated pairwise by at least $d_{\min}$, and 50 Monte Carlo episodes are run. The communication radius is $R_c = 40$ and the minimum separation is $d_{\min} = 3$. The assignment risk weight is $\gamma_r = 2.0$. For waypoint selection, up to $K = 36$ valid candidates are collected by rejection sampling: with probability 0.70, $c = (1-a)s_i + a\,\tilde{s}_i$ along the start–subgoal segment, and with probability 0.30, $c = (1-a)\tilde{s}_i + ag_i$ along the subgoal–goal segment, where $\tilde{s}_i$ is the guidance subgoal and $a \sim U(0,1)$; each candidate is then perturbed by isotropic Gaussian noise $\varepsilon \sim \mathcal{N}(0, \sigma^2 I)$ with $\sigma = 3$ and rounded to the nearest grid cell, rejecting obstacle, occupied, and reserved cells until 36 valid candidates are collected or a maximum of $30K = 1080$ sampling trials is reached, so the final candidate set may contain fewer than 36 points, and the guidance subgoal follows (7). The assignment-stage topology weight is w_T^{A}=1.0; for waypoint selection, w_L=0.30, w_R=0.15, w_T^{W}=0.15, and w_C=0.15. The reserved mask uses a window of radius $r = 2$ cells (a 5×5 neighborhood, i.e., $\eta = 25$). The assignment SA uses 1200 iterations with an initial temperature of 2.0 and a cooling rate of 0.995. All methods are implemented in MATLAB R2023b and executed on a PC equipped with an Intel Core i7-10750H CPU at 2.60 GHz and 16 GB RAM. A* operates on an 8-connected grid, with unit cost for horizontal/vertical moves and $\sqrt{2}$ for diagonal moves.

The proposed CTR is compared with (i) PP, a prioritized planning baseline that assigns the first N targets of the task pool to the UAVs by index order and plans the UAVs in ascending order of distance to

Table 1. Overall performance comparison.

Method	Succ.	Fail.	Conn.	$\overline{\lambda_2/N}$	Length (cells)	Energy (a.u.)	Makespan (steps)	Time (s)
PP	0.60	0.40	0.364	0.050	274.2	277.9	85.2	0.138
GA	0.84	0.16	0.242	0.028	164.0	166.6	51.5	0.113
CTR	0.89	0.11	0.343	0.059	161.4	164.7	48.7	0.103
CTR-NoTopo	0.89	0.11	0.228	0.026	159.9	163.2	48.6	0.035

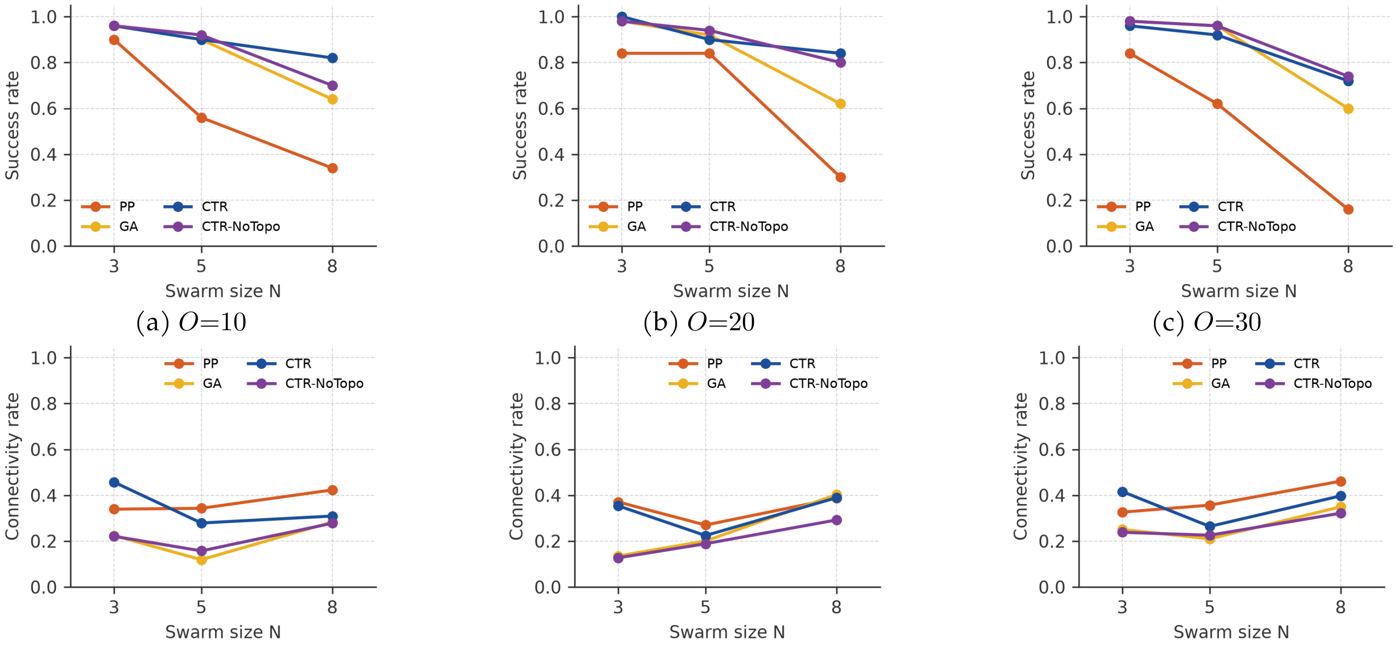

(a) O=10 (b) O=20 (c) O=30

(d) O=10 (e) O=20 (f) O=30

Figure 3. Success rate (top) and connectivity rate (bottom) versus swarm size under $O = 10$, 20, and 30 obstacles.

their targets using A* with a reserved mask and wait insertion; (ii) GA, a genetic-algorithm baseline whose chromosome encodes a permutation of the M targets, from which the first N targets are assigned to the UAVs; it uses a population of 60, 80 generations, order crossover, tournament selection ($k = 3$), and mutation probability 0.15, with a fitness that only includes distance and obstacle risk, and after assignment the paths are generated by the same A*, reserved mask, and wait insertion as CTR; and (iii) CTR-NoTopo, an ablation of CTR with the topology terms disabled.

An episode is successful if all UAVs reach their targets without any inter-UAV or obstacle collision; otherwise, the episode is regarded as failed, and by construction the success rate and the failure rate sum to one. Communication disconnection alone does not classify an episode as failed; connectivity is evaluated as a separate performance metric. Let T_e denote the makespan of episode e, i.e., the number of time steps of the longest valid UAV path, and let $I_{e,t} \in \{0, 1\}$ indicate whether the communication graph is connected at step t of episode e. The per-episode connectivity rate is defined as

$$C_e = \begin{cases} \frac{1}{T_e} \sum_{t=1}^{T_e} I_{e,t}, & T_e > 0, \\ 0, & T_e = 0, \end{cases}$$

and the overall connectivity rate is the equal average over episodes, $C_{\text{conn}} = \frac{1}{N_{\text{ep}}} \sum_{e=1}^{N_{\text{ep}}} C_e$. A UAV that has already reached its target is assumed to remain at the target position until the makespan; for a failed episode in which planning terminates before a valid path is generated for every UAV, T_e is set to the length of the longest valid path generated before termination, and each UAV without a valid planned path is held at its start position throughout this T_e-step horizon, with its communication links still evaluated according to (1); if no valid path is generated at all before termination, then $T_e = 0$, no time step is evaluated, and the definitions above assign $C_e = 0$ and $A_e = 0$ to that episode. The per-episode normalized algebraic connectivity is likewise defined as

$$A_e = \begin{cases} \frac{1}{T_e} \sum_{t=1}^{T_e} \frac{\lambda_{2,e,t}}{N}, & T_e > 0, \\ 0, & T_e = 0, \end{cases}$$

where $\lambda_{2,e,t}$ is the algebraic connectivity of the communication graph at step t of episode e, and its overall value is $\overline{\lambda_2/N} = \frac{1}{N_{\mathrm{ep}}}\sum_{e=1}^{N_{\mathrm{ep}}} A_e$. Path length is the total Euclidean path length summed over the UAVs that obtained a valid path, in grid units. A motion-energy proxy is defined as $E_{\mathrm{proxy}} = \ell + w_{\mathrm{turn}}\sum_t (1-\cos\theta_t)$, where ℓ is the path length, θ_t is the heading change at step t, and $w_{\mathrm{turn}} = 0.2$; the resulting quantity is reported in arbitrary units (a.u.). Makespan is the number of time steps of the longest valid UAV path. Time is the average planning (computation) time per episode, in seconds. The connectivity and normalized algebraic connectivity are computed over all episodes, whereas the trajectory-based metrics path length, energy proxy, and makespan are valid-path aggregates accumulated only over the UAVs that obtained a valid path and then averaged over all episodes; planning time is averaged over all episodes. Because these trajectory-based metrics omit UAVs with no valid path, they characterize the cost of the feasible portion of each episode rather than a strict per-UAV efficiency measure, and they should not be used to compare path efficiency across methods with substantially different failure rates.

4.2 Overall Performance

Figure 2 reports the average success rate, failure rate, connectivity rate, and normalized algebraic connectivity over all settings. CTR attains the highest algebraic connectivity among all methods and achieves a higher success rate and lower failure rate than PP and GA. Although PP exhibits a slightly higher connectivity rate than CTR, its normalized algebraic connectivity is lower; this indicates that the connectivity rate only measures whether the graph is connected, whereas λ_2/N further reflects the strength of the connected topology, so CTR favors more strongly coupled communication configurations rather than merely maximizing the fraction of connected time steps. Compared with the topology-ablated CTR-NoTopo, it substantially improves both the algebraic connectivity and the connectivity rate with essentially the same success rate, confirming that the topology guidance strengthens connectivity robustness without sacrificing success rate and with similar valid-path aggregate costs.

Table 1 summarizes the quantitative metrics defined above. In addition to the mission-success and connectivity metrics, relative to CTR-NoTopo, CTR only marginally increases path length, energy proxy, and makespan, while the additional topology evaluation increases the average planning time from 0.035 s to 0.103 s; nevertheless, the absolute planning time remains lower than that of PP (0.138 s) and GA (0.113 s) in the current implementation.

4.3 Effect of Obstacle Density and Swarm Size

Figure 3 shows the success rate and connectivity rate grouped by obstacle density. The topology terms help the swarm avoid disconnected configurations, and the topology-ablated variant CTR-NoTopo exhibits lower connectivity rates than CTR in most settings, confirming the overall benefit of the proposed topology guidance.

5 Conclusion

This paper presented a communication topology resilience-guided method for multi-UAV cooperative planning. By modeling the swarm communication graph through its weighted Laplacian and using the algebraic connectivity λ_2 as a global resilience objective, the proposed CTR method embeds topology awareness into both task assignment and waypoint selection. The assignment stage adds a spectral topology term, solved by simulated annealing, that directly rewards the algebraic connectivity of the selected targets, and the waypoint selection stage adds an isolation-penalty cost that reduces the risk of isolated UAVs mid-flight, followed by A* stitching and wait-insertion temporal correction. Simulation results demonstrate stronger algebraic connectivity together with a higher success rate than PP and GA, as well as substantial connectivity gains over the topology-ablated variant. Future research will focus on dynamic re-planning under communication failures and moving obstacles, adaptive topology-weight adjustment under time-varying network conditions, and validation in larger-scale swarm and hardware-in-the-loop scenarios.

Data Availability Statement

The data used to support the findings of this study are available from the corresponding author upon request.

Funding

This work was supported by the National Natural Science Foundation of China under Grant 62471204, and Jiangsu Provincial Key Research and Development Program under Grant BE2023022-2.

Conflicts of Interest

Quan Li served as an Editorial Board Member of the *Aerospace Engineering Communications* at the time of manuscript submission. To ensure the integrity of the peer-review process, Quan Li was not involved in the editorial handling, peer review, or decision-making process for this manuscript, which was handled independently by another editor. The remaining authors declare no conflicts of interest.

AI Use Statement

The authors declare that no generative AI was used in the preparation of this manuscript.

Ethical Approval and Consent to Participate

Not applicable.

References

[1] Chung, S. J., Paranjape, A. A., Dames, P., Shen, S., & Kumar, V. (2018). A Survey on Aerial Swarm Robotics. *IEEE Transactions on Robotics*, *34*(4), 837-855. [CrossRef]

[2] Yu, J., & LaValle, S. M. (2016). Optimal multirobot path planning on graphs: Complete algorithms and effective heuristics. *IEEE Transactions on Robotics*, *32*(5), 1163-1177. [CrossRef]

[3] Ma, H. (2022). Graph-Based Multi-Robot Path Finding and Planning. *Current Robotics Reports*, *3*(3), 77-84. [CrossRef]

[4] Van Den Berg, J. P., & Overmars, M. H. (2005, August). Prioritized motion planning for multiple robots. In *2005 IEEE/RSJ International Conference on Intelligent Robots and Systems* (pp. 430-435). IEEE. [CrossRef]

[5] Goldberg, D. E. (1989). *Genetic Algorithms in Search, Optimization, and Machine Learning*. Addison-Wesley. https://www2.fiit.stuba.sk/~kvasnicka/Free%20books/Goldberg_Genetic_Algorithms_in_Search.pdf

[6] Holland, J. H. (1992). Genetic Algorithms. *Scientific American*, *267*(1), 66-73. [CrossRef]

[7] Sharon, G., Stern, R., Felner, A., & Sturtevant, N. R. (2015). Conflict-Based Search for Optimal Multi-Agent Pathfinding. *Artificial Intelligence*, *219*, 40-66. [CrossRef]

[8] Choi, H. L., Brunet, L., & How, J. P. (2009). Consensus-based decentralized auctions for robust task allocation. *IEEE transactions on robotics*, *25*(4), 912-926. [CrossRef]

[9] Zavlanos, M. M., & Pappas, G. J. (2008). Distributed Connectivity Control of Mobile Networks. *IEEE Transactions on Robotics*, *24*(6), 1416-1428. [CrossRef]

[10] Yun, W. J., Park, S., Kim, J., Shin, M., Jung, S., Mohaisen, D. A., & Kim, J.-H. (2022). Cooperative multiagent deep reinforcement learning for reliable surveillance via autonomous multi-UAV control. *IEEE Transactions on Industrial Informatics*, *18*(10), 7086-7096. [CrossRef]

[11] Kong, X., Zhou, Y., Li, Z., & Wang, S. (2024). Multi-UAV simultaneous target assignment and path planning based on deep reinforcement learning in dynamic multiple obstacles environments. *Frontiers in Neurorobotics*, *17*, 1302898. [CrossRef]

[12] Westheider, J., Rückin, J., & Popović, M. (2023, October). Multi-UAV adaptive path planning using deep reinforcement learning. In *2023 IEEE/RSJ international conference on intelligent robots and systems (IROS)* (pp. 649-656). IEEE. [CrossRef]

[13] Puente-Castro, A., Rivero, D., Pedrosa, E., Pereira, A., Lau, N., & Fernandez-Blanco, E. (2024). Q-Learning Based System for Path Planning with Unmanned Aerial Vehicles Swarms in Obstacle Environments. *Expert Systems with Applications*, *235*, 121240. [CrossRef]

[14] Kim, Y., & Mesbahi, M. (2005, June). On maximizing the second smallest eigenvalue of a state-dependent graph Laplacian. In *Proceedings of the 2005 American Control Conference* (pp. 99-103). IEEE. [CrossRef]

[15] Xie, H., Yang, D., Xiao, L., & Lyu, J. (2021). Connectivity-aware 3D UAV path design with deep reinforcement learning. *IEEE Transactions on Vehicular Technology*, *70*(12), 13022-13034. [CrossRef]

[16] Yanmaz, E., Balanji, H. M., & Güven, İ. (2024). Dynamic multi-UAV path planning for multi-target search and connectivity. *IEEE Transactions on Vehicular Technology*, *73*(7), 10516-10528. [CrossRef]

[17] Savkin, A. V., Huang, C., & Ni, W. (2022). Joint multi-UAV path planning and LoS communication for mobile-edge computing in IoT networks with RISs. *IEEE Internet of Things Journal*, *10*(3), 2720-2727. [CrossRef]

[18] Meng, K., He, X., Wu, Q., & Li, D. (2023). Multi-UAV Collaborative Sensing and Communication: Joint Task Allocation and Power Optimization. *IEEE Transactions on Wireless Communications*, *22*(6), 4232-4246. [CrossRef]

[19] Kirkpatrick, S., Gelatt Jr, C. D., & Vecchi, M. P. (1983). Optimization by simulated annealing. *science*, *220*(4598), 671-680. [CrossRef]

[20] Fiedler, M. (1973). Algebraic Connectivity of Graphs. *Czechoslovak Mathematical Journal*, *23*(2), 298-305. [CrossRef]

[21] Olfati-Saber, R., Fax, J. A., & Murray, R. M. (2007). Consensus and Cooperation in Networked Multi-Agent Systems. *Proceedings of the IEEE*, *95*(1), 215-233. [CrossRef]

Quan Li received the Ph.D. degree in Control Science and Engineering from Jiangnan University, Wuxi 214122, Jiangsu, China, in 2025. (Email: quanli_1124@163.com)

Zitong Shen is currently pursuing the B.Sc. degree at Jiangsu Second Normal University, Nanjing 211222, Jiangsu, China. (Email: shenzitong1217@163.com)

Qingwen Ding is currently pursuing the B.Sc. degree at Jiangsu Second Normal University, Nanjing 211222, Jiangsu, China. (Email: 1548349595@qq.com)

Yaxuan Liu received the Ph.D. degree from Nanjing University of Posts and Telecommunications, Nanjing, Jiangsu, China, in 2025. (Email: carol_liuyx@163.com)

Rui Dai received the Ph.D. degree in Computer Science and Technology from Zhejiang University of Technology, Hangzhou 310014, Zhejiang, China, in 2025. (Email: jxdxdr@zjxu.edu.cn)

Jin Zhou received the B.Eng. degree in Computer Science and Technology from Southeast University, Nanjing, China. She is currently an Associate Dean and Senior Experimentalist with the School of Computer Engineering and School of Artificial Intelligence, Jiangsu Second Normal University. Her teaching and research interests include computer systems, undergraduate education, and student innovation training. She has published papers in core journals, led provincial and municipal research projects, and obtained invention patents and software copyrights. (Email: zhou@jssnu.edu.cn)

Yiyang Ni is a Professor and Dean of the School of Computer Engineering and School of Artificial Intelligence, Jiangsu Second Normal University, Nanjing, China, and a Ph.D. supervisor at Nanjing University of Posts and Telecommunications. He has led more than 30 research projects, published over 80 SCI/EI-indexed papers, and holds more than 30 granted Chinese invention patents. His research achievements have received multiple provincial- and national-level science and technology awards. (Email: niyy@jssnu.edu.cn)